

# THEORETICAL STUDY OF NONLINEAR CHATTER STABILITY ANALYSIS BASED ON SYNTHESIS OF LINEARIZATIONS IN OPERATING POINTS FOR DIFFERENT TURNING CONDITIONS

PETR HADRABA<sup>1</sup>, JIUNN-JYH WANG<sup>2</sup>, HUEI-MIN LIN<sup>2</sup>,  
ZDENEK HADAS<sup>1</sup>

<sup>1</sup>Brno University of Technology, Faculty of Mechanical  
Engineering, Brno, Czechia

<sup>2</sup>National Cheng Kung University, Department of  
Mechanical Engineering, Tainan, Taiwan

DOI: 10.17973/MMSJ.2022\_10\_2021083

*Petr.Hadraba@vutbr.cz*

This paper deals with an approach to study nonlinear chatter analysis, which is based on the synthesis of linear theory for different turning conditions. Mainly, contact nonlinearities play a crucial role in the behavior of the machine tool and the stability of turning operation. However, the analysis of nonlinear systems is challenging because nonlinear system analyzes are often limited to a linearized solution, which may be insufficient to reveal the stability lobe diagram. The presented study proposes a theoretical approach which is based on a synthesis of linearization in the operating point. This approach provides several solutions of stability lobe diagrams which are strongly depending on the loading conditions of the nonlinear system and all solutions are integrated to the final stability lobe diagram. The presented method is applied to a simplified 2D structure between two supports with nonlinear contact stiffness. Resulted analysis of the lobe diagram are compared with results of the time-domain simulations and it shows a good match. This paper shows that the presented approach offers an effective solution for refining the stability estimate for nonlinear mechanical systems.

## KEYWORDS

Chatter, nonlinear system, contact, linearization, machine tool, stability lobe diagram.

## 1 INTRODUCTION

Dynamic nonlinearities highly influence machine tool behavior. This fact is well known and often observed during experimental measurements. However, most of the machine structure analysis considers only linear behavior and nonlinear parameters are neglected or linearized around the operation point. The main reason is avoiding time-consuming nonlinear analysis and linearization of mechanical system around the operation point commonly provide an effective tool for prediction dynamic operation. In the case of turning operation, this approach is suitable for the definition of a conservative minimum limit of stable chip width. However, according to chatter stability theory [Stephenson2018], the minimum limit width stability criterion

("unconditional stability" region) is too limiting, and there are large stable areas above this criterion ("conditional stability") for most machine tools. The main problem is that linear analysis does not fittingly describe these areas [Hadraba 2020]. Naturally, machine structures are nonlinear due to nonlinearity in the mechanical joints [Dhupia 2007, Ding 2013]. The question is not if they are nonlinear but how strong that the nonlinearity is. And could we predict the change of stability lobe diagram in case of strong nonlinearity of machine tool structure? For this reason, this paper adopts the well-known chatter theory and analysis of stability lobe diagram. Thereafter, the results of this theory were used for different nonlinear characteristics of assumed systems and the synthesis of all results provided a new improved lobe diagram.

Modern machine tools are often based on ball-groove contact mechanisms with preload linear ball guideways and ball screws; these mechanical joints are based on nonlinear ball groove contact [Johnson 1987]. Therefore, many researchers describe the behavior of these components; Dolata presents an experimental analysis describing the nonlinear behavior of ball-screw stiffness [Dolata 2015]. The experimental modal analysis of the linear ball guideway presents Ohta [Ohta 2000], evaluating the proportion of contact stiffness and carriage stiffness. The main emphasis is on modeling and losing preload in the vertical direction influenced by contact nonlinearity [Shaw 2013, Ohta 2010]. Li focuses on the transient phase of the ball's influence on the vertical vibration performance [Li 2020].

In contrast to many works that consider only vertical stiffness, Wu focuses on bending loads [Wu 2012]. The volume of linear ball guideway contact preload impacts its behavior; Lin analyzes how the CNC milling machines' dynamic behavior changes depending on the linear ball guideway's preload [Lin 2010]. Hung describes the shift of the chatter stability depending on preload [Hung 2011]; the simplified model of nonlinear stiffness of the linear ball guideway presented in this paper is based on a similar model presented in works [Wang 2018, Wang 2019]. Wang analyzes how the load affects the positioning table based on a linear ball guideway. These presented findings conclude that it is necessary to analyze the machine tool stability while considering the preload, linear ball guideway and the total load applied to the mechanism.

According to these findings, it is necessary to develop an effective method for nonlinear contact analysis, mainly in the case of determination accurate stability lobe diagram. This paper presents an approach based on the synthesis of linearization in the operating points algorithm (SLOP). The algorithm aims to offer an effective way to analyze the chatter stability of structures based on a linear ball guideway. The results of the algorithm are presented on a simple 2D structure example — a rigid beam supported by two linear ball guideways. A time-domain simulation was used for simulation results validation. SLOP's main advantage is its time efficiency, whereby it can analyze a broader range of conditions but reduce the time a hundred times compared to the time-domain simulation.

## 2 MOTIVATION

The multi-spindle lathes have high productivity requirements; therefore, its slides must enable the grooving process with high chip width and feed --which means high chatter stability under high loads. However, under these conditions, the nonlinearities in the mechanical joints of the structure occur, which leads to chatter stability estimation problem. The problem is that there is no "simple" method for analyzing nonlinear structures and the effect of nonlinearity on machine tool structures. The fast chatter analysis for machine tools with nonlinear behavior is

highly required. The prediction of chatter and stability analysis, shown in Fig. 1, has the dual importance in both phases, machine tool life – design and operation. Firstly, it has a crucial role in machine tool design; it is necessary for machine structure optimization of the guideway layout. Secondly, it is important to design the appropriate conditions for stable machining.

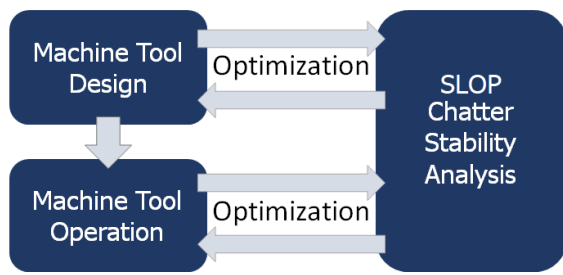


Figure 1. Chatter Stability Analysis in machine tool life cycle

The nonlinearities in mechanical joints are easily observed from modal hammer measurements, where the amplitude and width of the force impulse causes the system's different responses. Inputs and responses in Fig. 2 and Fig. 3 show that the structure changes its behavior depending on the deflection. However, this measurement only points on the space around the equilibrium position. It is almost impossible to obtain dynamic characteristics under static loading. Therefore, the only possibility is directly testing the cutting conditions, but the results of these experiments are not transferable to other conditions. This is highly inconvenient, mainly during the development of a new prototype, because before the actual structure is produced, there is just insufficient knowledge about the final dynamics. The other problem is that some machines behave according to the linear theory, but in the same chip width with different speeds they behave like two different machines with a similar force load.

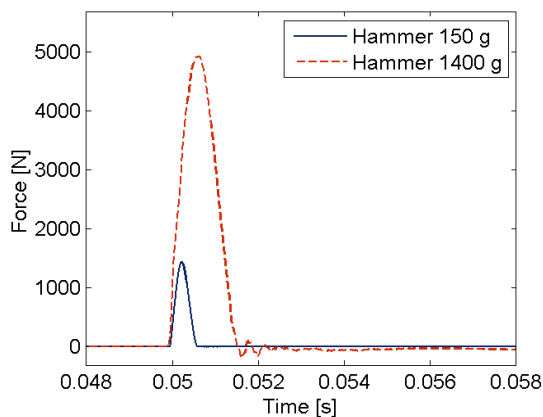


Figure 2. Impulses of modal hammer with different mass and tip materials

The description of these mechanical structures with structural nonlinearities in early development is needed. One option is using a time-domain simulation for analyzing of mechanical structure. However, the time-domain simulation is time-consuming. Thus, it is necessary to develop a fast and effective method that enables an approximately mapping of the machining condition.

SLOP algorithm could answer this problem which combines the structure's local linearization under static load and calculate a linearized lobe diagram under many operation points, which could answer this problem. It enables the use of a nonlinear static analysis instead of time-domain simulation. What is necessary to know is the type of nonlinearity in the mechanical joint, for instance, in a linear ball guideway, some producers also present force-deflection diagrams of their boundaries. The presented 2D model provides the simplest mechanical model,

which could enable the simulation of the parallel solution for the same chip width and for this reason it was chosen for the presentation of this approach to efficient calculation of nonlinear stability lobe diagrams.

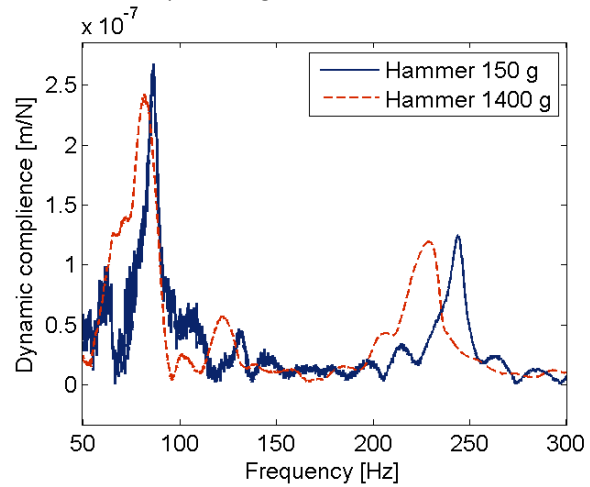


Figure 3. Response of a system based on linear ball guides after being struck by different modal hammers

### 3 REGENERATIVE CHATTER

Chatter is a type of self-excited vibration; the paradox is that this vibration is not the additional necessary energy flow, but the machining process itself generates the energy exciting the vibration. Gegg describes in the publication [Gegg 2011] the simple principle of regenerative chatter; this model could be seen in Fig. 4. The knife cuts the material, and because of the stiffness structure which connects it to the surrounding work, the waves remain on the surface. In the first turn, it is its natural frequency placement. In the next step, the tool interacts with the waves from the previous cut and depends on the face shift between the continuing and previous cut; the vibration is forced or calmed down.

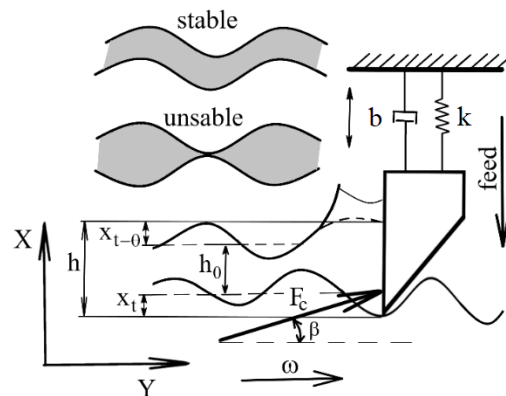


Figure 4. Simple scheme of regenerative chatter model

The key is to define conditions when the system is stable and unstable; Tlustý in the publication [Tlustý 2000] defined them by a limit width of the chip  $b_{lim}$  as a fraction, where the specific cutting force  $K_s$  and the negative real part of the system's transfer function  $G(u)$  are in the denominator:

$$b_{lim} = \frac{-1}{2 K_s \text{real}(G(u))} \quad (1)$$

If we consider a minimum of the negative real function  $\min(G(u))$ , we get the whole spindle speed stability criterion. However, this criterion is too strict, so the next step in the classical analysis is to define the phase shift  $\varepsilon$ , which is the inverse tangent of the fraction of the real and imaginary part of the transfer function:

$$\epsilon = \text{atan} \left( \frac{\text{real}(G(u))}{\text{imag}(G(u))} \right). \quad (2)$$

The last step before building the lobe diagram is to calculate the reaction frequency  $f_{ri}$  for each harmonic lobe. Where  $f_s$  represents the spindle speed and  $N$  is a series of systems harmonics

$$f_{r_i} = \left( N + \frac{\epsilon}{2\pi} \right) f_s; \quad N = 1, 2, 3 \dots n. \quad (3)$$

Combining the reaction frequency with the limit stable chip width, we get a stability lobe diagram; this diagram draws the boundary between the stable and unstable conditions. The typical stability lobe diagram can be seen in Fig. 5, this stability lobe diagram corresponds to the following structure linearized under 50 N cutting force load.

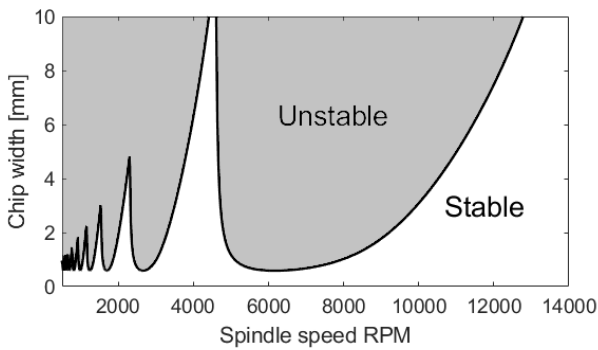


Figure 5. Lobe diagram divides the machining condition into stable and unstable

Chatter is a nonlinear phenomenon, dependent on many secondary processes [Wiercigroch 2001]. Therefore, many works extend the basic theory by these influences. One of these influences is process damping, which increases stability in the low-speed range [Elias 2017] [Fu 2014]. Nonlinear behavior can be caused by coupling seemingly independent modes in the cutting process [Beri 2018]. Workpiece stiffness often plays a significant role in vibration stability, so it is sometimes necessary to include it in a general vibration analysis [Chen 2006].

#### 4 NONLINEAR STIFFNESS MODEL OF LINEAR BALL GUIDEWAY WITH PRELOAD

A typical example of nonlinearity in mechanical joints represents a linear ball guideway. Due to the combination of preload and nonlinear stiffness of a ball groove contact, the whole linear ball guideway system's nonlinearity is relatively high and causes changes in chatter stability. The behavior can be easily described by the Hertzian contact between a ball and a groove contact. The simplest model is usually represented by a two-ball groove contact with a preload. Sun and Kong present this kind of model and use experimental validation to prove its behavior [Sun 2013], [Sun 2015]. In the following work, Kong extends and presents a polynomial approximation of linear ball guideway stiffness [Kong 2015]. These more advanced models also consider the angular relations in the linear ball guideway. However, these models are too complicated, and the primary behavior matches the simple Hertzian contact model. The equation describes the basic Hertz's contact model of the linear ball guideway stiffness:

$$F(x) \begin{cases} k \cdot ((x_0 + x)^{3/2} - (x_0 - x)^{3/2}) & x < x_0 \\ k \cdot (x_0 + x)^{3/2} & x > x_0 \\ -k \cdot (x_0 - x)^{3/2} & x < -x_0. \end{cases} \quad (4)$$

Where  $F$  is the reaction force of the contact,  $x_0$  is the displacement caused by preload,  $k$  is the stiffness coefficient,

and  $x$  is the deflection from the guideway's equilibrium position. The stiffness dramatically changes around the boundary of the preload loss. If we consider that the loss of preload happens when one row of the ball-groove contact has a double preload deflection and the other is without any deflection, then we can define the contact loss load  $F_l$  as the proportion of preload force  $F_p$ :

$$F_p = k \cdot x_0^{3/2}, \quad (5)$$

$$F_l = F_p \cdot \frac{(2x_0)^{3/2}}{x_0^{3/2}} = F_p \cdot 2^{3/2}. \quad (6)$$

Manufacturers usually declare the load of lost preload to be  $2.8 F_p$ . The parameters are preload force  $F_p = 140$  N and nonlinear stiffness coefficient  $k = 7.55e9$  N/m<sup>3/2</sup>. For these conditions, we get the resulting dependence of stiffness on deflection in Fig.8, where there is a noticeable region with stiffness decreasing by 30 %.

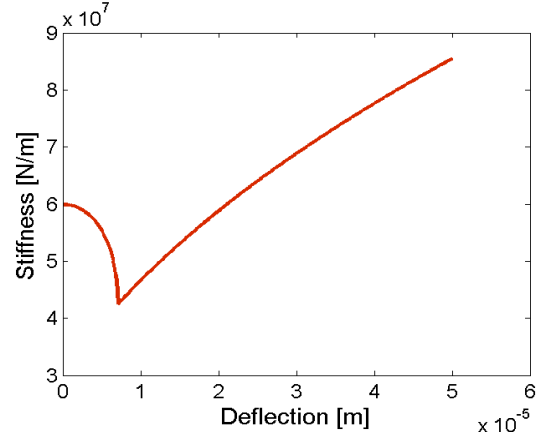


Figure 6. Stiffness dependency of models on the deflection

#### 5 MACHINE TOOL SLIDE MODEL FOR STABILITY ANALYSIS

##### 5.1 Proposed 2D model of a typical grooving operation

The simulation model is inspired by an engineering problem of turning machine, where the cutting tool is damaged during a typical turning operation. It is caused by regenerative chatter in a theoretically stable area. As was mentioned above, there are parallel solutions for the same chip width and for this reason this situation is analyzed by the models which allow their parallel solutions.

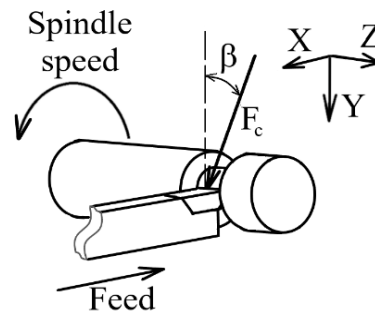


Figure 7. Principle of grooving operation

The proposed approach is presented on the chatter stability analysis of a typical grooving operation. Fig. 7 shows a scheme of the grooving process with the cutting force orientation. The cutting force lies in the plain XY, where also lies the feed direction, which is oriented in the -X direction. A model of this grooving operation could be simplified as a two-dimensional problem, where the mechanical structure consists of a rigid beam and a flexible support with two spring joints. The scheme of the model is shown in Fig. 8. The first mode of this model under load could be responsible for the losing of stability and

chatter behavior. However, the model has a degree of freedom in the Y direction; but we assume a 2D model and we consider movement only in the X direction and rotation in the Z-axis. The model is a rigid body represented by its weight and momentum of inertia in the center of gravity. This body is joined by two linear ball guideways which are represented by two nonlinear spring-damper models.

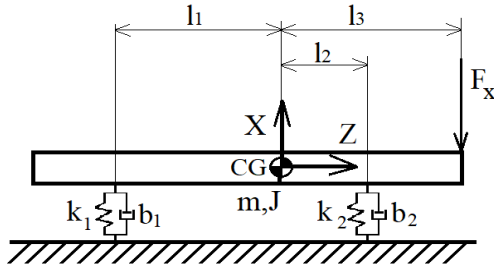


Figure 8. Model of structure with parallel spring system

Regarding the previous assumptions, the model is represented by its momentum of inertia by two differential equations. The first represents the center of gravity's displacement in the X direction, and the second describes its rotation displacement.

$$m\ddot{x} = -k_1(x - l_1\theta) - k_2(x + l_2\theta) - b_1(\dot{x} - l_1\dot{\theta}) - b_2(\dot{x} + l_2\dot{\theta}) + F, \quad (7)$$

$$J\ddot{\theta} = k_1(x - l_1\theta)l_1 - k_2(x + l_2\theta)l_2 + b_1(\dot{x} - l_1\dot{\theta})l_1 - b_2(\dot{x} + l_2\dot{\theta})l_2 + Fl_3. \quad (8)$$

By transforming equations 4 and 5 to the matrix form, we get the metrics  $\mathbf{M}$ ,  $\mathbf{K}$ ,  $\mathbf{B}$ , and the force vector  $F$ :

$$\mathbf{M} = \begin{bmatrix} m & 0 \\ 0 & J \end{bmatrix} \quad (9)$$

$$\mathbf{K} = \begin{bmatrix} k_1 + k_2 & -k_1l_1 + k_2l_2 \\ -k_1l_1 + k_2l_2 & -k_1l_1^2 + k_2l_2^2 \end{bmatrix} \quad (10)$$

$$\mathbf{B} = \begin{bmatrix} b_1 + b_2 & -b_1l_1 + b_2l_2 \\ -b_1l_1 + b_2l_2 & -b_1l_1^2 + b_2l_2^2 \end{bmatrix} \quad (11)$$

$$F = \begin{pmatrix} 1 \\ l_3 \end{pmatrix} \quad (12)$$

Equation 10 provides the solution to the deflection and rotation of center of gravity  $x_{CG}$ , which depends on the angular speed of the harmonic force vector:

$$x_{CG}(\omega) = (\mathbf{K} - \omega^2\mathbf{M} + i\omega\mathbf{B})^{-1}F \quad (13)$$

For a stability analysis, it is necessary to get a solution under the force. The total deflection combines rotation and translation of the center of gravity:

$$x_F(\omega) = [1, l_3] x_{CG}(\omega) \quad (14)$$

Damping parameters  $b_1$ ,  $b_2$  are represented by a simple linear model. The value of the damping coefficient was chosen to reach approximately 3% of the critical damping for both modes for the linear structure. However, due to the nonlinear stiffness, the proportion of damping is changing. The damping coefficient and the rest of the parameters except stiffness are in Tab. 1 The stiffness of the springs is defined by the nonlinear model described above.

$m$	$J$	$l_1$	$l_2$	$l_3$	$b_1, b_2$
85 kg	6 kgm <sup>2</sup>	210 mm	20 mm	140 mm	6·10 <sup>-3</sup> Nm <sup>-1</sup> s

Table 1. Parameters for the presented linear model

The possibility of future development of the model is the replacement of the rigid beam with a flexible system. One of the possible approaches is described by Hadas in the publication [Hadas 2012], where he describes the problem of using elastic components in mechatronic models. As a result, this device allows the creation of complex nonlinear models. However, in our illustrative example, we will be satisfied with a simplified model.

## 5.2 Static analysis of this 2D structure

In the future, for the chatter estimation, it is necessary to analyze a static solution first. It is because we assume that the chatter starts from the smooth surface. The presented system is statically definite, so we can use momentum and force equilibrium equations to define the force in each boundary and depend on the load.

$$F_1 = F \cdot \frac{(l_3 - l_2)}{(l_1 + l_2)} \doteq 0.522 \cdot F \quad (15)$$

$$F_2 = -F \cdot \left(1 + \frac{l_3 - l_2}{l_1 + l_2}\right) \doteq -1.522 \cdot F \quad (16)$$

From the values above, it is evident that the force in the second spring  $k_2$  is almost three times higher than in the first spring  $k_1$ . This fact means that the reaction of  $k_2$  has a crucial role in chatter stability. With the assumption of small angles, the total deformation of the system under a load can be defined by the equation:

$$x = \left(\frac{f_{k_1}(F_1) + f_{k_2}(F_2)}{l_1 + l_2}\right) \cdot (l_3 - l_2) + f_{k_3}(F_2) \quad (17)$$

## 5.3 Simplified grooving time-domain simulation model

The time-domain analysis for the validation of SLOP follows the previous research focused on the simulation of chatter stability of nonlinear structures [Hadraba 2020]. The topological description of the simulation is provided in Fig. 9.

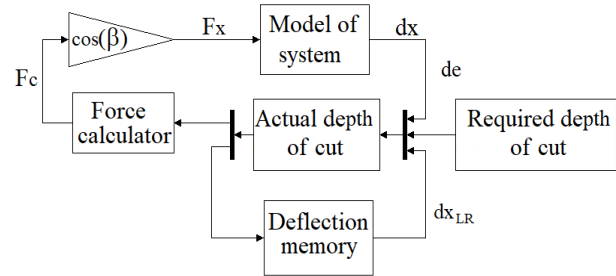


Figure 9. The scheme of simulation model for regenerative chatter used for simulation

The central part is the structure's dynamic model with force input and deflection output. The information of knife deflection is sent to the block with another two inputs. The required depth of the cut and deflection in the previous rotation. The output of this block is the actual cut's depth. This value divides it into two ways; one runs into the memory stored for the next turn, the other flows into the force calculator. As a cutting force is split into the x-direction according to the constant cutting angle  $\beta$  and finally comes back in the central part. The force calculator represents the specific cutting force coefficient  $K_s$  and the chip width. To compare, each simulation is necessary to have an exact material removal. In this grooving operation, we simulate the grooving depth which corresponds to 60 rotations. The values of all used parameters are included in Tab. 2.

Feed	$K_s$	$\beta$	Groove depth
0.04 mm/rev	3500 MPa	30 deg	2.4 mm

Table 2. Parameters for time-domain simulation

This basic simulation scheme could be extended by the spindle dynamic cut's deep dependent specific cutting force; also, multidirectional inputs could be included, these extensions of the simulation model present previous work [Hadraba2018]. However, for a clear comparison between SLOP would these extensions be overcomplicated.

Three different solvers were used:

- Ode5 fifth order Dormand-Prince formula,
- Ode8 eighth order Dormand-Prince formula,



- Ode14x Newton's method and extrapolation combination.

The most precise solver is ode14x; however, it also needs more steps. The simulation step was  $5e-5$  s, which enables an accurate computation for all their solvers. The small computational step is necessary not only due to the numerical computation but also to allow a fine division of the circumference during high spindle speed simulation. The duration of the simulation corresponds to 60 revolutions. The range of simulations is 3000-6000 rpm with a step of 15 rpm and the range of chip width from 0.5 mm to 5 mm with a step of 25  $\mu$ m. In total, there are 9191 time-domain simulations of the system. The maximum amplitude and frequency of vibrations are analyzed in the following range.

## 6 PROPOSED SLOP ALGORITHM FOR PRECISE STABILITY CHATTER ANALYSIS OF STRUCTURE WITH NONLINEAR STIFFNESS

The main idea of the SLOP algorithm is that the nonlinear structure under different loads has a unique set of linearized stiffness. Hence, it would also have a different stability lobe diagram. Fig. 10 shows the case of three different loads corresponding to different chip widths (each stability lobe diagram is valid only for a specific chip width) and the figure shows these areas as blue-stable and gray-unstable stripes. The final stability lobe diagram is composed of many of these local solutions; the total number depends on the required accuracy and the stability lobe diagram range.

The assumption for the local linearization synthesis is that the chatter starts from a smooth surface with no other interruptions. According to this, the start of instability depends on the local behavior of the system. This is the reason we can split the task of the lobe diagram into several subanalysis, and then the results of the local stability prediction are combined into one lobe diagram.

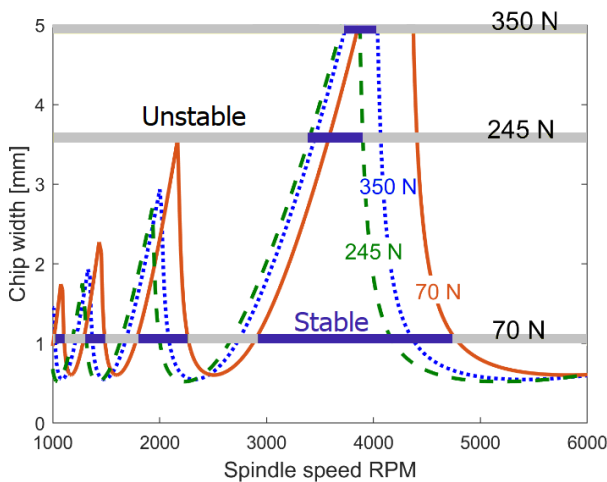


Figure 10. An example of the operation of the SLOP: three linearized stability lobe diagrams for different load segments corresponding to the chip width form the final stability lobe diagram

This algorithm aims at a fast detection of possible instability in the structure with height structural stiffness nonlinearities. The principle is to decompose the stability assumption problem into several subproblems. The first step is to define a range of stability analysis and evaluate the cutting force applied during the stable machining process. After that, the nonlinear static analyses are applied to each of these loads. This analysis's required outputs are the stiffnesses of each connector, which is a linearization of each of these solutions. Before evaluating the system's general stability, the unstable solutions are excluded due to their transient behavior. Then, the unique sets of linearized stiffness combinations are used to create the matrix  $K$

(equation 7) and compute a linear solution following equations 10 and 12. This solution is used for a classical chatter analysis according to equations: (1) – (3).

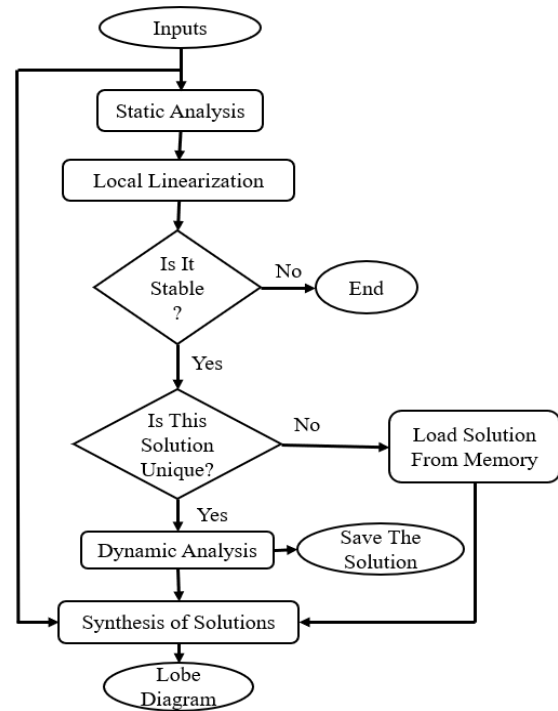


Figure 11. Scheme of the proposed SLOP algorithm

The algorithm assumes that operations with bifurcations can exist in the structure, so there could be more than one stable solution for typical loading conditions, and all these unique solutions must be analyzed. The analysis of all these solutions is done and the synthesis of all these possible solutions are compounded into a new improved general lobe diagram.

## 7 RESULTS AND DISCUSSION

### 7.1 Dynamic response of simulated impact response

As we showed in the motivation part, real mechanical structures could provide different responses in the case of nonlinear stiffness. Such responses are occurred during the modal hammer measurement, where different amplitudes of hits cause changes in the dynamic system response. Such structural nonlinearities could play a significant role in chatter stability behavior. Therefore, the time-domain simulation of the impact response was applied to the presented nonlinear responses of the analyzed mechanical structure to verify its behavior.

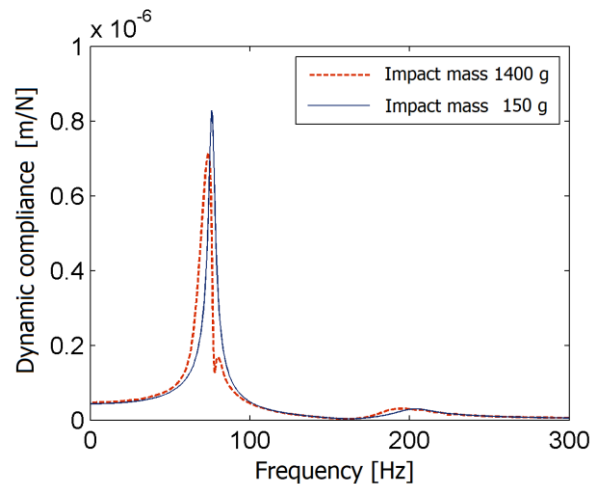


Figure 12. Simulated impact response

The real input signals of the force the signals, e.g., signals shown in Fig. 2, were applied to analyze the simulated mechanical structure. The simulation results show that the system response depends on the impact. The simulated deflection signal is transformed by the Fast Fourier transform (FFT) into the frequency domain and the resulting dynamic compliance is shown in Fig. 12, where information such as modal frequency peaks, and shape modes are included. Hence, the presented model could represent the frequency peak shift and the change in the frequency domain peak shape. It should be noted that this simulation model does not correspond to the measured of real machine structure from Fig. 3, which should only illustrate the chatter stability problem and the peak amplitudes are not intentionally tuned. However, transformation of the structural model into the planar 2D mechanism (with chosen parameters of the simulation model) could provide appropriate results, mainly in the case of illustration for the presented approach of effective chatter stability analysis.

### 7.2 Comparison of SLOP lobe diagram with time-domain simulation

The results of time-domain simulation are shown in Fig. 13. The presented 3D graph shows the maximal knife amplitudes, which are affected by the nonlinear characteristics of the presented model. The results resemble a steep cliff from the front edge of the instability (lobe edge which is defined by the system's range from natural frequency to min real part range) and sloping down to the back edge of the instability (lobe edge which is defined by the spectrum above min real part range). Below the 2 mm chip width, the highest amplitude ridge follows the edge of the stable system; above it bends towards lower speeds where at its minimum point it changes the trend, and with higher chip width it grows towards higher speeds.

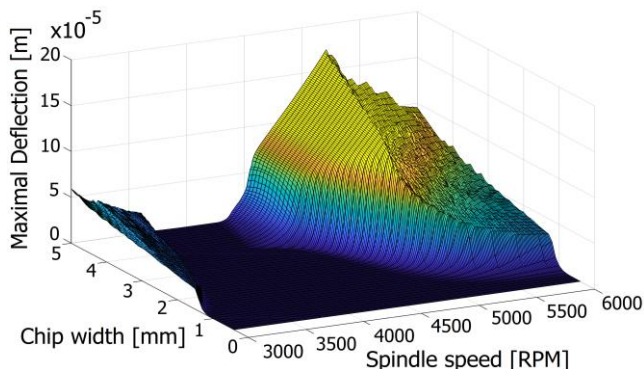


Figure 13. Time-domain simulation detection of maximal deflection depending on the chip width and spindle speed

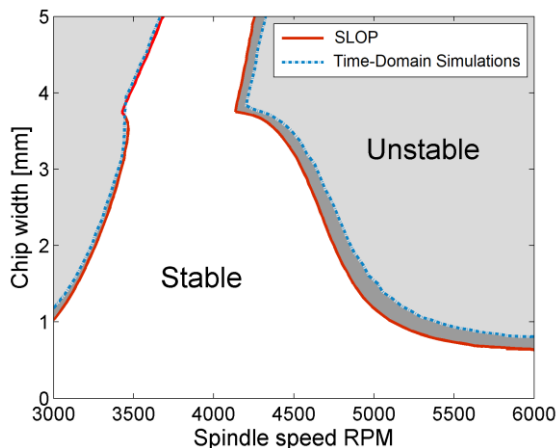


Figure 14. Comparison of time-domain simulation and SLOP estimation of chatter stability lobe diagram

The projection of the stable and unstable region and comparison with the SLOP results are shown in Fig. 14. The results of both SLOP and time-domain simulations show that even the system based on the Hertzian contact theory causes noticeable changes in the chatter stability. For both results, we can notice the front side's deformation approximately in the lobes, mainly in the area from 3 mm to 4 mm chip width where the stability drops to the lower spindle speed; above this area, the trend changes, and the lobe's edge is deformed following the higher speed. However, the SLOP solution provides a more conservative stability estimation. The backside of the lobe provides different results, wherein the results above 2.5 mm chip width time-domain simulation offer better results.

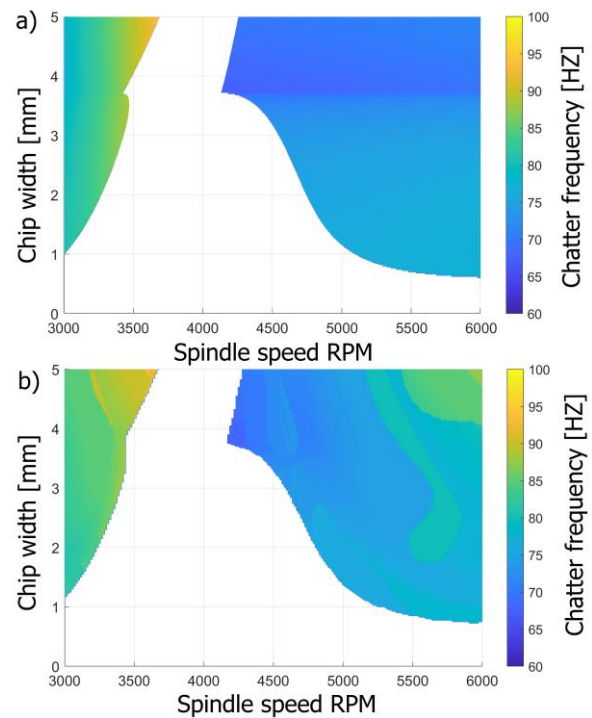


Figure 15. Comparison of frequency maps estimated by SLOP algorithm (a) and time-domain simulation (b)

The chatter frequency maps in Fig. 15 show that the frequencies match well only on the edge of stability. Due to high instability inside the lobe body, the linearization does not match the simulation. The main reason is that these regions do not satisfy the quasi-static deflection assumption; hence their instantaneous stiffness value cannot be generally linearized. This fact is the reason for the resulting deviation in the predicted frequency map.

An important parameter is the time required for the analysis. Tab. 3 presents the time spent on SLOP and time-domain simulation with three different solvers. The resolution (speed step 12 RPM, chip width 0.05 mm) and the analyzed space are the same, which corresponds to Fig. 14. The time-domain simulation without the ode14x, ode8, ode5 solvers takes, respectively, one month, two weeks, and a week.

SLOP	Time Domain Simulation		
	Ode14x	Ode8	Ode5
5857 s	$2.432 \times 10^6$ s	$1.1578 \times 10^6$ s	$5.4923 \times 10^5$ s

Table 3. Required time for SLOP and Time-domain analysis simulation with three different solvers

In contrast to this, the SLOP takes 90 minutes, which means that SLOP is significantly more time effective, mainly for large-scale evaluation. The possible way to speed up a time-domain

simulation is to stop the simulation after the chatter is detected, which decreases the time spent by 60 %. Another possible way to decrease the time spent is to use a heuristic algorithm oriented to instability edge detection. However, this reduces the information of the system. The highest SLOP time spent (above 95 %) is the final step of the algorithm, the processing of lobe boundaries: resampling and identifying stability and instability.

### 7.3 Feed dependent stability lobe diagram

The feed is usually a neglected parameter in the chatter stability analysis. However, if the stiffness depends on the load, the feed becomes an important parameter with a significant influence on the stability lobe diagram. Fig. 17 shows the stability lobe diagram dependency on the cutting force. Two waves caused by the stiffness drop in each spring, which bends the maximal stability to w-shape, are significant. This diagram is the basis of the SLOP where three individual sections are presented in Fig. 10.

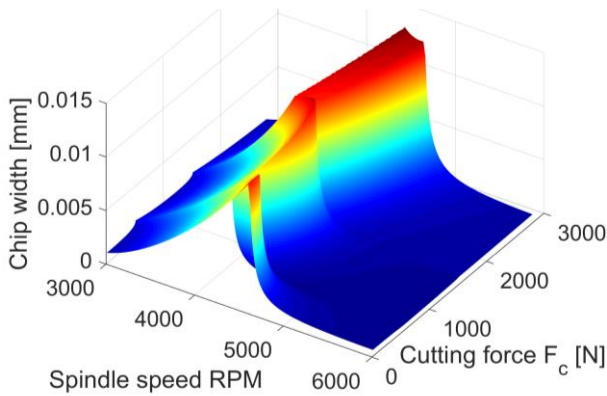


Figure 16. Surface created by individual linearized stability lobe diagrams dependent on spindle speed and cutting force

The advantage of SLOP is that one linearized data set can be used for another stability lobe diagram with different feed parameters; this makes the whole process quite effective. The set of linearization space must be only extended if the required load exceeds the current maximum of the linearized set.

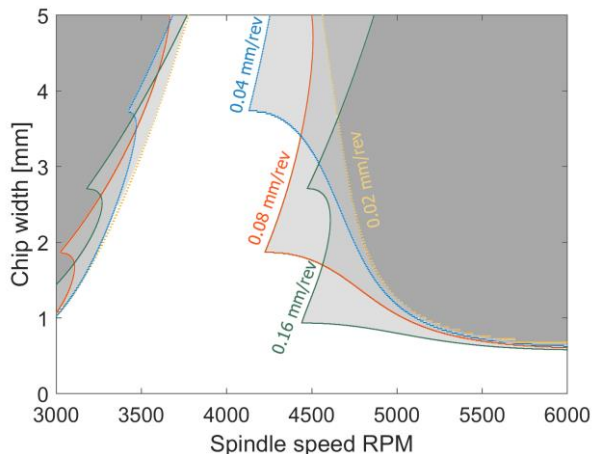


Figure 17. Comparison of stability lobe diagram estimated by SLOP algorithm for different feeds

Four different feed stability lobe diagrams created by SLOP are presented in Fig. 17. It is noticeable that the lobe edge follows the trend from Fig. 16; in the highest load feed 0.16 mm/rev, we could see a full deformed W-shape edge. The trend is obvious — higher feed causes the stability lobe diagram W-deformation due to the lower chip width, in contrast to the low load, which moves it to higher chip width. The feed 0.02 mm/rev looks almost like a linear stability lobe diagram; however, it is caused by the shift of the deformed area above the observed area. Broadening the view of the matter will provide us with Fig. 18

which shows a comparison of SLOP stability lobe diagram (for 0.04 mm/rev) with a linear alternative (red line). It shows a good match in the low-speed area where the neighboring lobes meet before the significant deformation happens. Therefore, the spindle speed range and the stiffness drop should be considered before the analysis.

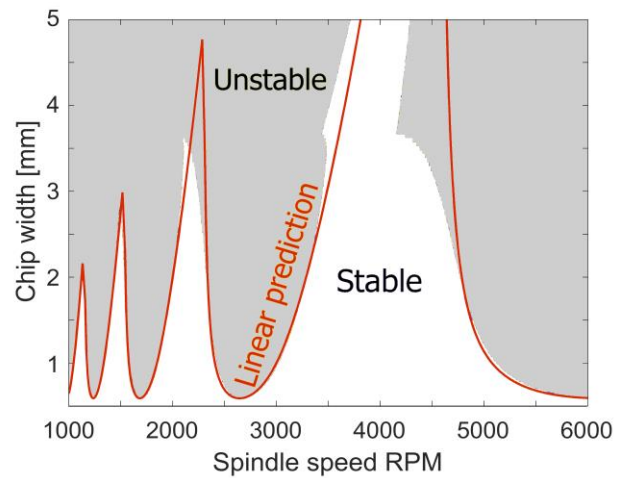


Figure 18. Comparison of stability lobe diagram estimated by SLOP algorithm and linear system stability lobe diagram in the wider speed range

The presented results of SLOP show a good match with time-domain simulation. Nevertheless, this example is simplified, and many parameters were neglected. Often the values of coefficients vary depending on the unknown parameters. Due to this fact, it is necessary to approach the chatter stability problem as a stochastic system. Furthermore, the application of the SLOP to actual machine tool systems with experimental measurements is highly required for future development.

## 8 CONCLUSION

This paper proposes the SLOP algorithm, which provides the practical approach to determine stability lobe diagrams. The algorithm is based on a synthesis of linearization and enables chatter stability prediction. SLOP is applied to a simple mechanical structure with two nonlinear joints representing the linear ball guideway. This approach compared the SLOP algorithm with time-domain analysis on the presented 2D model of grooving operation. The results show that both approaches match, and the deviation between time-domain simulation and SLOP algorithm is not essential, both the primary trend and position of the lobes match.

These results prove that SLOP could be used for the chatter stability prediction for nonlinear behavior structures. Moreover, the speed of SLOP algorithm enables analyzing a larger space of cutting condition variation in a shorter time. Another advantage of SLOP algorithm is creating multiple stability lobe diagrams depending on the feed, which has a key role of stability in nonlinear structures.

The presented results also show that nonlinearity seriously changes the chatter stability and should be considered during machine tool development cycle. The structural nonlinearities of machines are not usually considered under the stability analysis, which could cause misinterpretation of experimental modal analysis and experimental stability analysis. Future developments should apply SLOP to a real machine tool structure to prove its functionality and validate the expected SLOP results with experimental measurements. Generally, machine tool analysis should focus more on flexible joint behavior.

## ACKNOWLEDGMENTS

These results were obtained with the financial support of the Faculty of Mechanical Engineering, Brno University of Technology (grant no. FSI-S-20-6335).

## REFERENCES

- [Stephenson2018] Stephenson, D. A., and Agapiou J. S. Metal cutting theory and practice, CRC press, 2018, ISBN 9781315373119
- [Hadraba 2020] Hadraba, P. and Hadas, Z. Time-Domain Regenerative Chatter Analysis of Non-linear Stiffness System. In: R. Szweczyk, ed. Mechatronics 2019: Recent Advances Towards Industry 4.0, 2020, pp. 3-10. ISBN 978-3-030-29993-4
- [Dhupia2007] Dhupia, J., Bartosz, P., Ulsoy, A. and Katz, R., Effect of a Nonlinear Joint on the Dynamic Performance of a Machine Tool. Journal of Manufacturing Science and Engineering, 2007, Vol. 129
- [Ding2013] Ding, W., Huang, X., and Wang, M. and Zhu, S., An approach to evaluate the effects of nonlinear traveling joints on dynamic behavior of large machine tools. The International Journal of Advanced Manufacturing Technology, 2013, Vol. 68
- [Johnson1985] Johnson K., Contact Mechanics. Cambridge University Press, 1987, ISBN 9781139171731
- [Dolata 2015] Dolata, M. and Jastrzebski, D. Identification of the parameters of a ball-screw mechanism model. Archives of Mechanical Technology and Materials, 2015, Vol. 35
- [Ohta 2000] Ohta, H. and Hayashi, E. Vibration of linear guideway type recirculating linear ball bearings. Journal of Sound and Vibration, 2000, Vol. 235, No. 5, pp 847-861. ISSN 0022460X
- [Shaw 2013] Shaw, D. and Su, W. L. Stiffness analysis of linear guideways without preload. Journal of Mechanics, 2013, Vol. 29, No. 2, pp 281-286. ISSN 17277191
- [Ohta 2010] Ohta, H. and Tanaka, K. Vertical stiffnesses of preloaded linear guideway type ball bearings incorporating the flexibility of the carriage and rail. Journal of Tribology, 2010, Vol. 132, No. 1, pp 1-9. ISSN 07424787
- [Li 2020] Li, C., Xu, M., He, G., Zhang, H., Liu, Z., and He, D. and Zhang, Y. Time-dependent nonlinear dynamic model for linear guideway with crowning. Tribology International, March 2020, Vol. 151 No. 5, pp 406-413. ISSN 0301679X
- [Wu 2012] Wu, J. S. S., Chang, J. Ch., Tsai, G. A., Lin, Ch. Y. and Ou, F. M. The effect of bending loads on the dynamic behaviors of a rolling guide. Journal of Mechanical Science and Technology, 2012, Vol. 26, No. 3, pp 671-680. ISSN 1738494X
- [Lin 2010] Lin, A. C. Y., Hung, J. P. and Lo, T. L. Effect of preload of linear guides on dynamic characteristics of a vertical column spindle system. International Journal of Machine Tools and Manufacture, 2010, Vol.50, No.8., pp 741-746. ISSN 08906955
- [Hung 2011] Hung, J. P., Lai, Y. L., Lin, C. Y. and Lo, T. L. Modeling the machining stability of a vertical milling machine under the influence of the preloaded linear guide. International Journal of Machine Tools and Manufacture, 2011, Vol.51, No.9., pp 731-739. ISSN 08906955
- [Wang 2018] Wang, W., Li, C., Zhou, Y., and Wang, H. and Zhang, Y. Nonlinear dynamic analysis for machine tool table system mounted on linear guides. Nonlinear Dynamics, 2018, Vol. 94, No. 3., pp 2033-2045. ISSN 1573269X
- [Wang 2019] Wang, W., Zhou, Y., and Wang, H., Li, C. and Zhang, Y. Vibration analysis of a coupled feed system with nonlinear kinematic joints. Mechanism and Machine Theory, 2019, Vol. 134, pp 562-581. ISSN 0094114X
- [Gegg 2011] Gegg, B.C., Suh, C.S. and Luo, A.C.J. Machine Tool Vibrations and Cutting Dynamics. Springer New York, 2011, ISBN 9781441998019
- [Tlustý 2000] Tlustý, G. Manufacturing Processes and Equipment, Prentice Hall, 2000, ISBN 9780201498653
- [Wiercigroch 2001] Wiercigroch, M. and Budak, E. Sources of nonlinearities, chatter generation and suppression in metal cutting, Philosophical Transactions of The Royal Society, 2001, Vol. 359, pp 663-693. ISSN 1471-2962
- [Elias 2017] Elias, S. and Matsagar, V. Research developments in vibration control of structures using passive tuned mass dampers. Annual Reviews in Control, 2017, Vol. 44, pp 129-156. ISSN 13675788
- [Fu 2014] Fu, Z., Zhang, X., Wang, X. and Yang, W. Analytical modeling of chatter vibration in orthogonal cutting using a predictive force model. International Journal of Mechanical Sciences, 2014, Vol. 88, pp 145-153. ISSN 00207403
- [Beri 2018] Beri, B. and Stepan, G. Stability of turning process with tool subjected to compression, Procedia CIRP, 2018, Vol. 77, pp 179-182. ISSN 2212-8271
- [Chen 2006] Chen, C. K., and Tsao, Y. M. A stability analysis of regenerative chatter in turning process without using tailstock. International Journal of Advanced Manufacturing Technology, 2006, Vol. 29, No. 7-8, pp 648-654. ISSN 02683768
- [Sun 2013] Sun, W., Kong, X. and Wang, B. Precise finite element modeling and analysis of dynamics of linear rolling guideway on supporting direction. Journal of Vibroengineering, 2013, Vol. 15, No. 3, pp 1330-1340. ISSN 13928716
- [Sun 2015] Sun, W. and Kong, X., Wang, B. and Li, X. Statics modeling and analysis of linear rolling guideway considering rolling balls contact. Proceedings of the Institution of Mechanical Engineers, Part C: Journal of Mechanical Engineering Science, 2015, Vol. 229, No. 1, pp 168-179. ISSN 20412983
- [Kong 2015] Kong, X., Sun, W., Wang, B. and Wen, B. Dynamic and stability analysis of the linear guide with time-varying, piecewise-nonlinear stiffness by multi-term incremental harmonic balance method. Journal of Sound and Vibration, 2015, Vol. 346, No. 1, pp 265-283. ISSN 10958568
- [Hadas 2012] Hadas, Z., Brezina T., Vetiska, J., and Brezina, L. Simulation modelling of mechatronic system with flexible parts. 2012 15th International Power Electronics and Motion Control Conference EPE/PEMC 2012 ISBN 978-1-4673-1971-3
- [Hadraba 2018] Hadraba, P. and Hadas, Z. Virtual Twin of The Multi-spindle Lathe for The Chatter Time-domain Analysis. Proceedings of the 2018 18th International Conference on Mechatronics – Mechatronika, Brno, 2018, pp 35-40. ISBN 978-80-214-5543-6.

## CONTACTS:

Ing. Petr Hadraba,  
Brno University of Technology, Faculty of Mechanical Engineering  
Technická 2896/2, 616 69 Brno, Czech Republic  
Petr.Hadraba@vutbr.cz